Available online at www.sciencedirect.com

ScienceDirect

IFAC PapersOnLine 52-26 (2019) 281–286

Extremum-Seeking for micro-algae biomass productivity maximization: an experimental validation

Christian G. Feudjio Letchindjio * **Laurent Dewasme** *
Alain Vande Wouwer *

* *Service d'Automatique, Université de Mons, Belgium.*
(e-mail: {ChristianGabin.FeudjioLetchindjio, Laurent.Dewasme, Alain.VandeWouwer}@umons.ac.be)

Abstract: This paper presents experimental results of a lab-scale implementation of an extremum seeking control strategy for maximizing the biomass productivity of cultures of the micro-algae *Dunaliella tertiolecta* in a flat-panel photobioreactor operated in continuous mode. The real-time optimization is based on a recursive least squares adaptation where the input (Dilution rate)/output (Biomass concentration) relation is approximated by a linear Hammerstein regression from which a productivity gradient estimate can be inferred. Lab-scale instrumentation and operating conditions are described and the results of two experiments are presented. They demonstrate the fast convergence of the extremum seeking scheme and practical considerations related to stability are discussed.

Keywords: Bioreactor, real-time optimization, micro-algae, extremum seeking control

1. INTRODUCTION

The race towards industrialization and the perpetual growth of the world population has increased fossil fuels global demand, and thus consumption, during the last decades. Nowadays, this fast depletion of fossil fuels reserves motivates the need for alternative and sustainable energy sources. Biofuels appear as an appealing solution to this problematic. They indeed encompass all fuels produced through biological processes and are classified in three categories depending on the source from which they are derived (Sengers et al., 2010). First generation biofuels are produced from food-crops (corn, sugar cane, vegetable oil...) and offer the advantage of an easy extraction process. However, their main drawbacks lie in the fact that extensive production requires large arable lands for crop cultivation and that their production is competing with human food-stock. On the other hand, second generation biofuels do not compete with human food-stock as they are produced from wasted and non-food materials but the bio-ethanol extraction process is more complicated in this case (Saladini et al., 2016). Third generation biofuels are produced from micro-algae, and have received ever increasing attention in the last two decades. Two main avenues can be followed with the production of lipids and subsequently, biodiesel via transesterification, or the production of starch, and subsequently bioethanol and biobutanol via fermentation. Besides, micro-algae have a handful of other applications including the production of high-value compounds of pharmaceutical interest, nutrients and pigments, CO_2 fixation and their use as tertiary step in wastewater treatment processes (Chisti, 2007; Abdel-Raouf et al., 2012).

Conventional control, such as PID, output-feedback linearization (Sbarciog et al., 2014) and model predictive control (Rawlings and Mayne, 2009) rely on the availability of a process model. However, bioprocesses are often only partially known and the inferred models complex and highly nonlinear. It might therefore be appealing to resort to model-free techniques, and also to develop dynamic optimization techniques that are directly in line with the production objectives, as for instance, the maximimization of algal biomass production in a photobioreactor (PBR). Extremum seeking offers such a perspective. In the well-known classical scheme, a bank of filters (BOF) is used to infer gradient information and an integrator drives this gradient to zero. However, the algorithm three-time scale separation remains its main limitation resulting in slow convergence (Ariyur and Krstic, 2003).

In (Dewasme et al., 2011), we have shown that a Recursive Least Square Extremum-Seeking (RLS-ES) strategy is able to improve the convergence speed by assuming an input/output linear static map. This technique is also developed in (Guay and Dochain, 2015). In (Feudjio Letchindjio et al., 2018), we further demonstrate that RLS-ES with plant dynamics under the form of a Wiener-Hammerstein representation, as originally introduced in (Moase and Manzie, 2011), outperforms the BOF- and static RLS-ES schemes.

Even though many theoretical studies of ES schemes are available in the literature, real-life applications remain relatively rare. The objective of this study is precisely to present such experimental validation of a RLS-ES strategy applied to cultures of *Dunaliella tertiolecta* in a flat-panel photobioreactor (PBR) operated in continuous mode.

2405-8963 © 2019, IFAC (International Federation of Automatic Control) Hosting by Elsevier Ltd. All rights reserved.
Peer review under responsibility of International Federation of Automatic Control.
10.1016/j.ifacol.2019.12.271

This paper is organized as follows. The first section introduces micro-algae culture modeling and control in PBR. The second section briefly presents the considered RLS-ES algorithm and control strategy. The third section describes the experimental set-up and instrumentation. Experimental results obtained with a lab-scale flat-panel PBR are discussed in section 5 while the last section draws conclusions and perspectives.

2. MICROALGAE CULTURES

Micro-algae growth is driven by photosynthesis. Light is used to enhance high-value compounds synthesis through CO_2 fixation and the assimilation of some basic nutrients (mainly Nitrogen and Phosphorus). Scale-up production can be achieved outdoor with large open pond raceways or indoor using PBRs (tubular, helicoidal or flat). However, outdoor productivity is limited (Mairet et al., 2015) due to the uncontrolled environment with fluctuations in the operating conditions (light intensity, temperature, pH,...) and the risk of contamination. On the other hand, PBR culture allows improving the monitoring and control of the operating condition controls and, as a result, the productivity at smaller scale than raceway ponds.

In conventional control strategies, a mathematical model can be used to predict the process behavior, and to infer optimal operating conditions. Droop (1968) introduced a macroscopic model uncoupling substrate (S ≡ Nitrogen) uptake and biomass (X) growth through the introduction of an intermediate stat, i.e., the internal quota (Q). This quota represents the portion of Nitrogen that is stored inside the cell and intended for growth. However, this model is restricted to constant light intensity and temperature conditions. Bernard (2011) proposed an extension accounting for varying light conditions, validated with experimental data from *Isochrysis Galbana* cultures in PBRs. The same model has been used for modelling *Scenedesmus Obliquus* cultures in tubular PBRs (Deschênes and Vande Wouwer, 2016). The model reads:

$$\begin{cases} \dot{X} = \mu X - DX - RX \\ \dot{S} = -\rho X + D(S_{in} - S) \\ \dot{Q} = \rho - \mu Q \\ \dot{I}^* = \delta\mu(\bar{I} - I^*) \end{cases} \tag{1}$$

with:

$$\begin{aligned} \rho &= \rho(Q, S) \\ \mu &= \mu(X, Q, I^*) \end{aligned}$$

where D, I^*, S_{in} respectively represent the dilution rate, the light intensity at which micro-algae are photo-acclimated and the inlet substrate concentration. Details about the growth rate μ and uptake rate ρ are discussed in (Bernard, 2011).

3. RLS-ES SCHEME

This section describes the basic principle of the control scheme presented in (Feudjio Letchindjio et al., 2018).

Assuming a linear Hammerstein model between the biomass and the dilution rate, the state-space equations are given by:

$$\begin{cases} X(k) = m\, D(k) + b & \text{(2a)} \\ X_f(k) = KX(k) - \beta_1 X_f(k-1) - \beta_2 X_f(k-2) & \text{(2b)} \end{cases}$$

where X_f is a filtered version of the signal X processed through a 2^{nd} order low-pass filter with unitary steady-gain ($K = 1+\beta_1+\beta_2$). The first pole accounts for biomass and sensor dynamics, while the second pole is used for noise attenuation.

Biomass productivity is defined as

$$P = D\,X \tag{3}$$

and the gradient estimate is given by:

$$\begin{aligned} \widehat{\frac{\partial P}{\partial D}} &= \frac{\widehat{\partial D\,X}}{\partial D} = \widehat{X} + D\,\frac{\widehat{\partial X}}{\partial D} \\ &= \widehat{X} + D\;\widehat{m} = 2\,\widehat{m}\,D + \widehat{b} \end{aligned} \tag{4}$$

where X has been replaced in (4) by its estimate $\widehat{X}$ computed following (2a) using the available parameter estimates at time k.

Alternatively, a filtered biomass productivity can be defined as:

$$P_f = D\,X_f \tag{5}$$

In this case, the gradient estimation can be computed following:

$$\begin{aligned} \widehat{\frac{\partial P_f}{\partial D}} &= \frac{\widehat{\partial D\,X_f}}{\partial D} = X_f + D\,\frac{\widehat{\partial X_f}}{\partial D} \\ &= X_f + D\frac{\widehat{\partial X_f}}{\partial X}\,\frac{\widehat{\partial X}}{\partial D} \\ &= X_f + D\widehat{\gamma}(k)\;\widehat{m} \end{aligned} \tag{6}$$

where an estimation of $\gamma(k)$ is obtained as:

$$\widehat{\gamma}(k) = \frac{X_f(k)}{\widehat{m}D(k) + \widehat{b}} \tag{7}$$

Both definitions lead in practice to the same performance, the filtering impact being included in the second case through $\widehat{\gamma}$. In the experimental study, we choose the second approach as X_f is directly available.

The control scheme is depicted in Fig. 1. A RLS algorithm estimates model (2) parameters from which productivity gradient estimate can be inferred following (6). The latter is then pushed to zero thanks to an integrator generating the suitable dilution rate to drive the productivity to its maximum value (at the optimum where $\widehat{\frac{\partial P}{\partial D}} = 0$). k_i is the integrator gain setting the closed-loop settling time. Besides, a sinusoidal dither signal $d(k)$ is added to the computed dilution rate to ensure persistency of excitation, i.e., to guarantee the convergence of closed-loop parameter estimation (Forssell and Ljung, 1999). The reader may refer to (Feudjio Letchindjio et al., 2018) for further details about the estimation algorithm implementation.

Note that the estimated *optimal* (in the sense of ESC) productivity and dilution rate can be inferred from (4) using (2a) - (3) as:

$$\widehat{\frac{\partial P}{\partial D}} = 2\,\widehat{m}\,D^* + \widehat{b} = 0 \implies \begin{cases} \widehat{D}^* = -\frac{\widehat{b}}{2\widehat{m}} \\ \widehat{P}^* = -\frac{\widehat{b}^2}{4\widehat{m}} \end{cases} \tag{8}$$

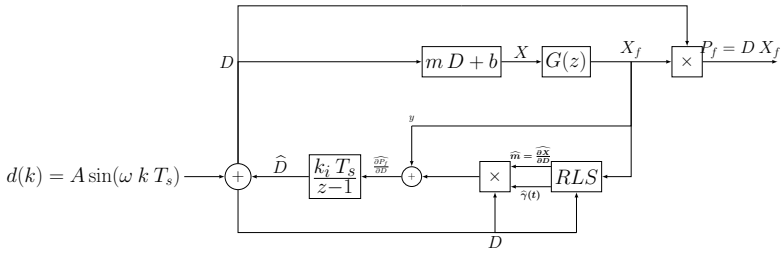

Fig. 1. ES scheme with RLS estimator with forgetting factor.

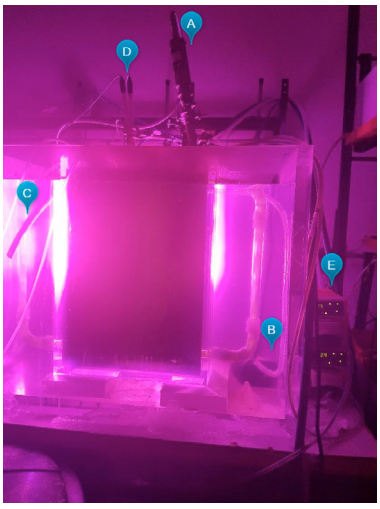

Fig. 2. Experimental lab-scale Photobioreactor

4. LAB-SCALE PBR AND EXPERIMENTAL SET-UP

Figiure 2 shows the lab-scale PBR and some of the core components of the installation. The micro-algae strain *Dunaliella tertiolecta* (19/6B) was obtained from Culture Collection of Algae and Protozoa SAMS Limited Scottish Marine Institute (CCAP) and a modified Johnson medium (Johnson et al., 1968) is used during the experiments. An Optek ASD19-N probe (see Fig. 2 - A) combined with a Fermenter Control HW-A1 provides an in-line real-time measurement of biomass by means of Near Infrared Range (NIR) absorption. This probe measures precisely the cell growth as a function of NIR absorption ($840-910\ nm$). It is made of stainless steel which allows durable and sanitary conditions as well as autoclaving. Figure 3 displays the calibration curve drawn between the Optek probe measurements and biomass dry weight from sampling.

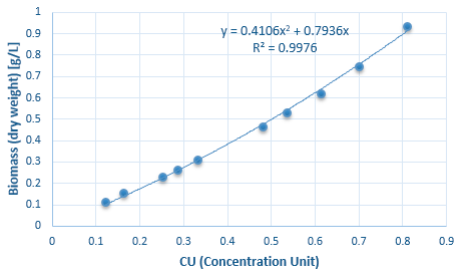

Fig. 3. Calibration curve between Optek probe measurements (CU) and biomass dry weight

The air-lift principle is used on both sides of the reactor to maximize the culture homogeneity. It has to be noticed that the Optek probe is put close to a recirculating PBR arm in order to avoid micro-algae accumulation on the probe which may cause biased measurements. The PBR is immersed in a water-bath whose temperature is regulated using a TEKO TK-500 Chiller/Heater ($T = 0-35$°C). An immersed pump (see Fig. 2 - B) circulates the water through the chiller and back to the water-bath (see Fig. 2 - C). An EI-1034 probe is used to sense the PBR medium temperature. Furthermore, the incident light is generated with a LumiGrow Pro 325 Horticultural Light Fixture. The latter contains LED lights producing more red and blue in the essential PAR ($400-700$ nm) range than the most powerful conventional systems in the industry, including any HID fixture. Apogee SQ-100 quantum sensors are used to measure the light intensity at the PBR surface. A PI controller has been designed to regulate the average incident light intensity on the PBR surface.

pH is measured with a pH probe (see Fig. 2 - D) and regulated by CO_2 injection using a BL 931700 mini pH control module. Continuous mode operation is achieved using 2 peristaltic Watson-Marlow pumps $120U$ for the dilution rate regulation (inflow & outflow, see Fig. 2 - E). Data acquisition is performed using Labjack cards and the control algorithm is run on LabView platform for real-time computation.

5. EXPERIMENTAL RESULTS

Two real-time experiments are conducted in order to validate the proposed RLS-ES strategy introduced in section 3. The first experiment lasts 10 days and the second one less than 5 days. The sampling period is chosen as $T_s = 0.01\ d = 14.4\ min$ to match simulation conditions in (Feudjio Letchindjio et al., 2018).

5.1 Experiment 1

The culture is first let to settle while maintaining a constant dilution rate $D(0) = 0.2\ d^{-1}$. The inlet substrate concentration is $S_{in} = 0.03\ gN.L^{-1}$, the average incident light $I_{av} = 300\ \mu Em^{-2}s^{-1}$, the temperature kept around $T = 24$°C and $pH = 7.1$. Extremum seeking control is activated once biomass concentration, and therefore the process, reaches steady-state (around $X(0) = 0.9\ gX.L^{-1}$), with the intergrator gain $k_i = 0.1$, $r = 1$ and $k_{trace} = 100$ for the constant trace algorithm (see Feudjio Letchindjio et al. (2018) for details). Biomass measurements are low-pass filtered prior to their use in the control algorithm

with a low-past filter of the form $G_{att}(z^{-1}) = \frac{1-a_{att}}{1-a_{att}z^{-1}}$ with $a_{att} = 0.9$.

Figure 4 shows that the biomass productivity and dilution rate reach their respective optimal estimated steady state values $\widehat{P}^* \approx 0.34\ gX.L^{-1}.d^{-1}$ and $\widehat{D}^* \approx 0.63\ d^{-1}$ approximately after 4 days following the control activation. The variations of X and D respectively shown in Fig. 4 and Fig. 5 allow the productivity P to reach the neighbourhood of the estimated optimum within 2 days thanks to a beneficial balance effect ($P = D\ X$).

The estimated gradient evolution is shown in Fig. 6. The latter confirms that the gradient is pushed to zero after 4 days thanks to the integrator action, and remains in a close neighbourhood of 0 during the rest of the experiment. Figure 7 displays the algorithm convergence diagram and the estimated static map computed using the parameter estimates (see Fig. 8). It is possible to build the estimated quadratic static map identified at each iteration k using (2a) - (3) for a dilution rate span (e.g $D \in [0\ 0.7]$) as :

$$\widehat{P}_{map} = \widehat{m}(k)\, D^2 + \widehat{b}(k)\, D \tag{9}$$

Furthermore, Figure 7 shows that at least 3 operating points belong to the estimated static map: the implicit steady-point $(0, 0)$, the starting point $\approx (0.2\ d^{-1}, 0.18\ gX.L^{-1}d^{-1})$ - recalling that the system was first let to settle prior the control activation - and the estimated optimum $(\widehat{D_1}^*, \widehat{P_1}^*) \approx (0.63\ d^{-1}, 0.34\ gX.L^{-1}.d^{-1})$. This observation supports the scheme convergence and the hypothesis that a quadratic static map may provide a good approximation of the real process map.

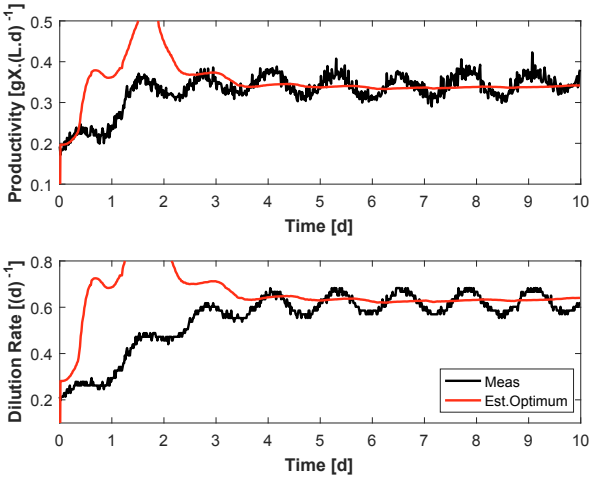

Fig. 4. Productivity and dilution rate evolution - experiment 1

5.2 Experiment 2

In the second experiment, different operating conditions are chosen in order to observe the effect of their variation on the optimum and assess the robustness of the proposed control strategy. As in experiment 1, the culture is first let to settle while maintaining a constant dilution rate $D(0) = 0.2\ d^{-1}$. The inlet substrate concentration is $S_{in} = 0.05\ gN.L^{-1}$, the average incident light $I_{av} = 800\ \mu Em^{-2}s^{-1}$, the temperature kept around $T = 30°C$

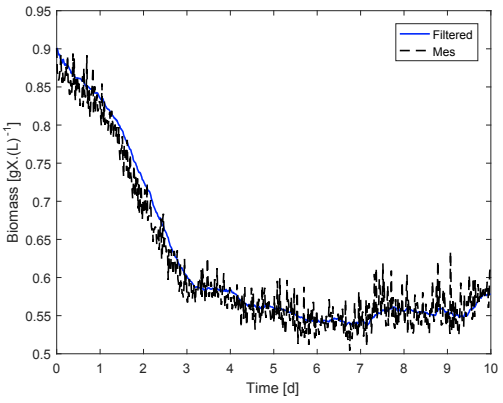

Fig. 5. Biomass concentration evolution - experiment 1

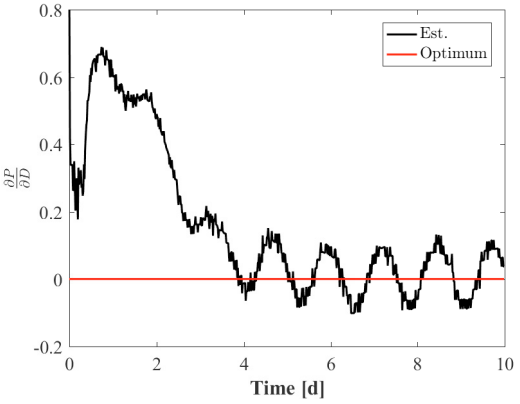

Fig. 6. Estimated gradient evolution - experiment 1

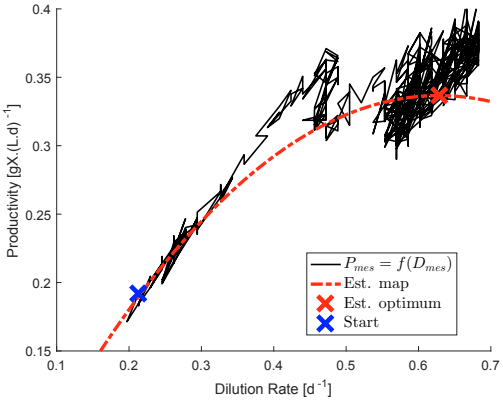

Fig. 7. Productivity/Dilution rate diagram along the experiment with estimated static map based on parameters estimates value on day 10 in (9) - experiment 1

and the pH is controlled around 7.1. The extremum seeking controller is activated once biomass concentration reaches steady-state (around $X(0) = 0.9\ gX.L^{-1}$). The integrator gain is changed to $k_i = 0.3$ to accelerate the convergence, $r = 1$ and $k_{trace} = 100$ for the constant trace algorithm. The low-pass filter is designed with $a_{att} = 0.95$ since the measurement noise is amplified, due to a voluntary increase of the air recirculation to improve

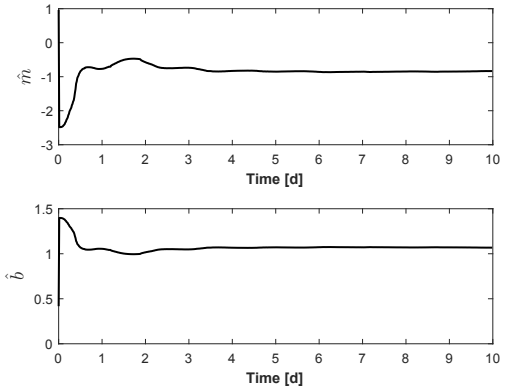

Fig. 8. Estimated static map parameters evolution - experiment 1

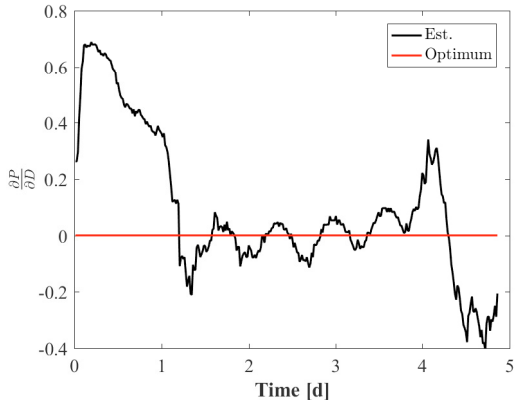

Fig. 9. Estimated gradient evolution - experiment 2

mixing (recalling that the Optek probe is near a PBR arm output as explained in Section 4).

Experimental results in Fig. 9 confirm that a higher integrator gain reduces the convergence time. Figures 9 and Fig 10 show that both productivity and dilution rate converge to their estimated optimal values after approximately 1 day. However, a drift of the estimated static map parameters is observed between $t \approx 3\ d$ and $t \approx 4\ d$ (see Fig. 11) resulting in a drift of the estimated optimal productivity and dilution rate values shown in Fig. 10. A possible explanation is the estimator wind-up (Astrom and Wittenmark, 1989; Sastry and Bodson, 1989; Isermann, 1982) due to a lack of*persistency of excitation* of the input signal. Estimator wind-up generally happens in steady-state operation. Solutions have already been proposed in the literature such as, for instance, adding a perturbation signal to the input (Gustavsson et al., 1977). However, the increase of the low-pass filter parameter a_{att} from 0.9 to 0.95, achieved in order to reduce the noise impact, may attenuate the informative content of the output and thus partially cancel the effect of the dither signal. From $t = 1.5\ d$ to $t = 4\ d$, very little oscillation is detected in the filtered biomass evolution (see Fig. 12), in contrast with the corresponding signal in Fig. 5 (first experiment). In (Feudjio et al., 2019), we propose a solution by combining the prefiltering with an extended estimator accounting for the presence of noise in the process model (RELS) to robustify the control structure in presence of high measurement noise levels.

Figure 13 shows that the optimum location moves with the operating conditions. In the 1^{st} experiment $(\widehat{D_1}^*, \widehat{P_1}^*) \approx (0.63\ d^{-1}, 0.34\ gX.L^{-1}.d^{-1})$ and in the 2^{nd} experiment $(\widehat{D_2}^*, \widehat{P_2}^*) \approx (0.8\ d^{-1}, 0.4\ gX.L^{-1}.d^{-1})$. The higher productivity achieved in Exp. 2 is in correlation with a higher inlet concentration ($S_{in2} = 0.05\ gN.L^{-1} > S_{in1} = 0.03\ gN.L^{-1}$) mitigating photo-inhibition effects due to higher incident light ($I_{av2} = 800\ \mu Em^{-2}s^{-1} > I_{av1} = 300\ \mu Em^{-2}s^{-1}$) (Bernard, 2011). Moreover, the experimental results obtained along these two different experiments are in accordance with the simulation results obtained with the reduced dynamic model of *Isochrysis galbana* in (Feudjio Letchindjio et al., 2018) where the optimal productivity for $I \in [100 - 200]\ \mu Em^{-2}s^{-1}$ lies between $0.35 - 0.6\ gX.L^{-1}.d^{-1}$.

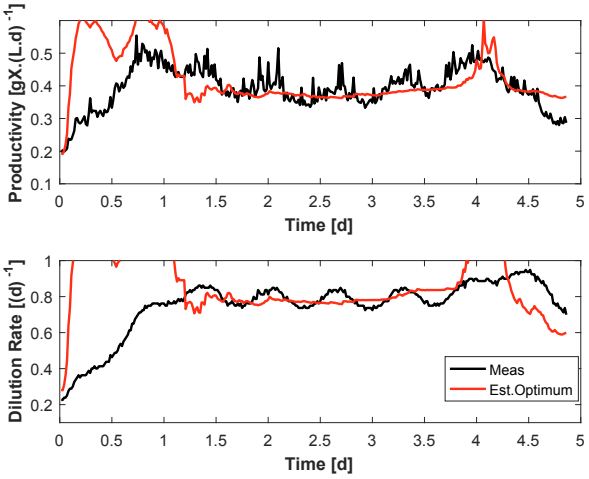

Fig. 10. Productivity and dilution rate evolution - experiment 2

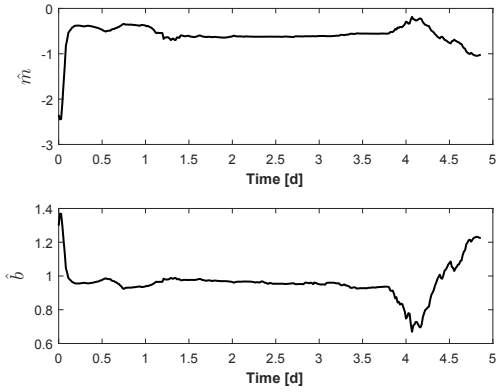

Fig. 11. Estimated static map parameters evolution - experiment 2

6. CONCLUSION

An experimental validation of a RLS-ES strategy maximizing biomass productivity in cultures of micro-algae *Dunaliella tertiolecta* in a lab-scale flat PBR, is presented. The convergence of the proposed real-time optimization scheme is fast, i.e., within a few days, and leads to expected optimal values for the productivity and the dilution

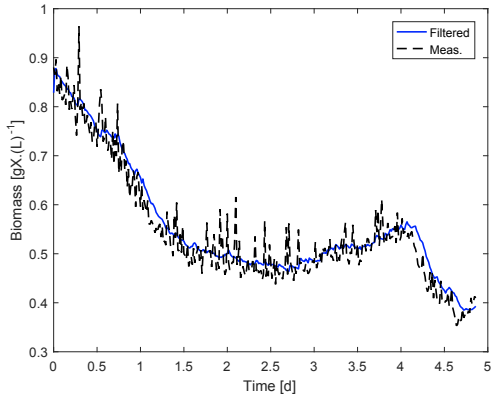

Fig. 12. Biomass concentration evolution - experiment 2

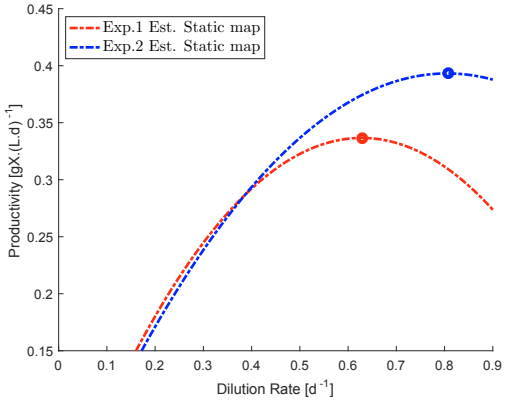

Fig. 13. Estimated static map and optimum from each of the 2 experiments. ● represents the estimated optimum (P^*, D^*)

rate (as compared to simulation results using a dynamic model). The experimental results show that an increase of the integrator gain may accelerate the convergence (the optimum may be reached in one day). However, these results also illustrate that some practical considerations need to be taken into account in order to guarantee closed-loop parameter identifiability and in turn closed-loop stability. In (Feudjio et al., 2019), we propose a solution to this latter issue and ongoing work is dedicated to the experimental validation of the improved strategy.

REFERENCES

Abdel-Raouf, N., Al-Homaidan, A., and Ibraheem, I. (2012). Microalgae and wastewater treatment. *Saudi journal of biological sciences*, 19(3), 257–275.

Ariyur, K.B. and Krstic, M. (2003). *Real-time Optimization by Extremum-seeking Control*. John Wiley & Sons, INC, wiley-interscience edition.

Astrom, K.J. and Wittenmark, B. (1989). *Adaptive Control*. Addison-Wesley. Prentice Hall.

Bernard, O. (2011). Hurdles and challenges for modelling and control of microalgae for co2 mitigation and biofuel production. *Journal of Process Control*, 21, 1378–1389.

Chisti, Y. (2007). Biodiesel from microalgae. *Biotechnology advances*, 25(3), 294–306.

Deschênes, J.S. and Vande Wouwer, A. (2016). Parameter identification of a dynamic model of cultures of microalgae scenedesmus obliquus-an experimental study. *IFAC-PapersOnLine*, 49(7), 1050–1055.

Dewasme, L., Srinivasan, B., Perrier, M., and Vande Wouwer, A. (2011). Extremum-seeking algorithm design for fed-batch cultures of microorganisms with overflow metabolism. *Journal of Process Control*, 21(7), 1092–1104.

Droop, M. (1968). Vitamin b12 and marine ecology. iv. the kinetics of uptake, growth and inhibition in monochrysis lutheri. *J. Mar. Biol. Assoc. UK*, 48(3), 689–733.

Feudjio, C., Dewasme, L., Deschenes, J.S., and Vande Wouwer, A. (2019). A slope seeking-based approach for optimal and sub-optimal SISO process control: Application to microalgae culture. *IFAC-PapersOnLine*, 52(1), 370–375.

Feudjio Letchindjio, C.G., Deschenes, J.S., Dewasme, L., and Vande Wouwer, A. (2018). Extremum seeking based on a Hammerstein-Wiener representation. *IFAC-PapersOnLine*, 51(18), 744–749.

Forssell, U. and Ljung, L. (1999). Closed-loop identification revisited. *Automatica*, 35(7), 1215–1241.

Guay, M. and Dochain, D. (2015). A time-varying extremum-seeking control approach. *Automatica*, 51, 356–363.

Gustavsson, I., Ljung, L., and Söderström, T. (1977). Identification of processes in closed loopidentifiability and accuracy aspects. *Automatica*, 13(1), 59–75.

Isermann, R. (1982). Parameter adaptive control algorithms − a tutorial. *Automatica*, 18(5), 513–528.

Johnson, M.K., Johnson, E.J., MacElroy, R.D., Speer, H.L., and Bruff, B.S. (1968). Effects of salts on the halophilic alga dunaliella viridis. *Journal of bacteriology*, 95(4), 1461–1468.

Mairet, F., Muñoz-Tamayo, R., and Bernard, O. (2015). Adaptive control of light attenuation for optimizing microalgae production. *Journal of Process Control*, 30, 117–124.

Moase, W.H. and Manzie, C. (2011). Fast extremum-seeking on Hammerstein plants. *IFAC Proceedings Volumes*, 44(1), 108–113.

Rawlings, J.B. and Mayne, D.Q. (2009). *Model predictive control: Theory and design*. Nob Hill Pub.

Saladini, F., Patrizi, N., Pulselli, F.M., Marchettini, N., and Bastianoni, S. (2016). Guidelines for emergy evaluation of first, second and third generation biofuels. *Renewable and Sustainable Energy Reviews*, 66, 221–227.

Sastry, S. and Bodson, M. (1989). *Adaptive Control : Stability, Convergence and Robustness*. Prentice Hall Information and System Sciences Series. Prentice Hall, Englewood Cliffs, New Jersey, thomas kailath edition edition.

Sbarciog, M., Coutinho, D., and Wouwer, A.V. (2014). A simple output-feedback strategy for the control of perfused mammalian cell cultures. *Control Engineering Practice*, 32, 123–135.

Sengers, F., Raven, R.P., and Van Venrooij, A. (2010). From riches to rags: Biofuels, media discourses, and resistance to sustainable energy technologies. *Energy Policy*, 38(9), 5013–5027.